NUWC-NPT Technical Report 12,141
15 August 2013

Mechanics of Air-Inflated Drop-Stitch Fabric Panels Subject to Bending Loads

Paul V. Cavallaro
NUWC Division Newport

Christopher J. Hart
Navatek, Ltd.

Ali M. Sadegh
The City College of New York

Naval Undersea Warfare Center Division
Newport, Rhode Island

Approved for public release; distribution is unlimited.

PREFACE

This research was funded under a Cooperative Research and Development Agreement (CRADA) between the Naval Undersea Warfare Center (NUWC) Division Newport and Navatek, Ltd.

The technical reviewer was Geoffrey R. Moss (Code 1522).

The authors gratefully acknowledge Martin S. Leff and David B. Segala of NUWC Division Newport for their support in conducting the material level tests and Gary Proulx and Karen Buehler of the Army Natick Soldier Research, Development, and Engineering Center, Natick, MA, for their support in designing the test frame and performing the inflated-panel bending tests.

Reviewed and Approved: 15 August 2013

Kelly J. Ross
Head, Ranges, Engineering, and Analysis Department

REPORT DOCUMENTATION PAGE

Form Approved
OMB No. 0704-0188

The public reporting burden for this collection of information is estimated to average 1 hour per response, including the time for reviewing instructions, searching existing data sources, gathering and maintaining the data needed, and completing and reviewing the collection of information. Send comments regarding this burden estimate or any other aspect of this collection of information, including suggestions for reducing this burden, to Department of Defense, Washington Headquarters Services, Directorate for Information Operations and Reports (0704-0188), 1215 Jefferson Davis Highway, Suite 1204, Arlington, VA 22202-4302. Respondents should be aware that notwithstanding any other provision of law, no person shall be subject to any penalty for failing to comply with a collection of information if it does not display a currently valid OPM control number.
PLEASE DO NOT RETURN YOUR FORM TO THE ABOVE ADDRESS.

1. REPORT DATE (*DD-MM-YYYY*)	2. REPORT TYPE	3. DATES COVERED (*From – To*)
15-08-2013	Technical Report	

4. TITLE AND SUBTITLE

Mechanics of Air-Inflated Drop-Stitch Fabric Panels Subject to Bending Loads

5a. CONTRACT NUMBER

5b. GRANT NUMBER

5c. PROGRAM ELEMENT NUMBER

6. AUTHOR(S)

Paul V. Cavallaro
Christopher J. Hart
Ali M. Sadegh

5.d PROJECT NUMBER

5e. TASK NUMBER

5f. WORK UNIT NUMBER

7. PERFORMING ORGANIZATION NAME(S) AND ADDRESS(ES)

Naval Undersea Warfare Center Division
1176 Howell Street
Newport, RI 02841-1708

8. PERFORMING ORGANIZATION REPORT NUMBER

TR 12,141

9. SPONSORING/MONITORING AGENCY NAME(S) AND ADDRESS(ES)

Naval Undersea Warfare Center Division
1176 Howell Street
Newport, RI 02841-1708

10. SPONSORING/MONITOR'S ACRONYM
NUWC

11. SPONSORING/MONITORING REPORT NUMBER

12. DISTRIBUTION/AVAILABILITY STATEMENT

Approved for public release; distribution is unlimited.

13. SUPPLEMENTARY NOTES

14. ABSTRACT

Rapid deployability and mobility of lightweight structures, namely inflatable structures, are of growing significance to the military and space communities. When deployment and rigidity are driven by pressure (for example, air or fluid) and materials such as textiles, elastomers, and flexible composites are used for the structure, significant load-carrying capacity per unit weight (or per-unit stowed volume) can be achieved. Specifically, the pressurized air directly provides the stiffness to support structural loads, thus eliminating the requirement for heavy metal stiffeners that are used in conventional rigid structures.

The technologies, materials, and system behaviors for these inflatable structures, however, are not sufficiently understood. Furthermore, predictive performance and analysis methods and test standards have not been adequately established because the structural behaviors of inflatable fabric structures often involve coupled effects from inflation pressure such as fluid-structure interactions, thermo-mechanical coupling, and nonlinear constitutive responses of the fabrics—all of which can restrict the use of conventional design, analysis, and test methods.

The research documented in this report focuses on the mechanics of air-inflated drop-stitch fabric panels that are subject to bending loads. Both analytical and experimental methods are used: the results of experimental four-point bend tests conducted at various inflation pressures were used to validate the analytical method, and predicted and experimentally obtained data such as deflections, wrinkling onset moments, ultimate loads, and pressure changes were compared.

15. SUBJECT TERMS
Inflatable Structures Drop-Stitch Fabrics Finite Element Analysis Experimental Mechanics Technical Textiles

16. SECURITY CLASSIFICATION OF:			17. LIMITATION OF ABSTRACT	18. NUMBER OF PAGES	19a. NAME OF RESPONSIBLE PERSON
a. REPORT	b. ABSTRACT	c. THIS PAGE			Paul V. Cavallaro
Unclassified	Unclassified	Unclassified	SAR	30	19b. TELEPHONE NUMBER *(Include area code)* 401-832-5082

TABLE OF CONTENTS

LIST OF ILLUSTRATIONS

LIST OF ILLUSTRATIONS (Cont'd)

Figure **Page**

LIST OF TABLES

Table **Page**

LIST OF ABBREVIATIONS AND ACRONYMS

3-D	Three-dimensional
CRADA	Cooperative Research and Development Agreement
EBT	Euler beam theory
FOS	Factor of safety
FSI	Fluid-structure interaction
NUWC	Naval Undersea Warfare Center
PVC	Polyvinyl chloride
SDBT	Shear-deformable beam theory
SEM	Scanning electron microscopy

MECHANICS OF AIR-INFLATED DROP-STITCH FABRIC PANELS SUBJECT TO BENDING LOADS

1. INTRODUCTION

Air-inflated drop-stitch fabric panels, considered pretensioned structures, are particularly suited for use in structural applications requiring flat (planar) shapes. Recently, these lightweight panels have become an important complement to the military's dominantly used inflatable shapes such as cylindrical beams, arches, and spheres, thus extending the range of geometries for inflatable structures. Like the other inflatable shapes, air-inflated drop-stitch panels provide a fail-safe mechanism during overload conditions; that is, unlike traditional structures that can buckle and fracture, inflatable drop-stitch fabric structures simply wrinkle and collapse without damage to the fabric. Once the overload is removed, the structure regains its design shape and structural performance.

The technologies, materials, and system behaviors for air-inflated drop-stitch fabric panels, however, are not sufficiently understood. Furthermore, predictive performance and analysis methods and test standards are inadequate because the structural behaviors of inflatable fabric structures often involve coupled effects from inflation pressure such as fluid-structure interactions, thermo-mechanical coupling, and nonlinear constitutive responses of the fabrics—all of which can restrict the use of conventional design, analysis, and test methods. To date, most research performed on inflatable fabric structures has focused on beam and arch-like structures and the development of particular analytical, numerical, and experimental methods[1 – 8] for these shapes. Except for the recently published findings on three-point bending tests conducted on inflatable drop-stitch panels,[9 – 10] very little open-literature addresses the use of drop-stitch fabrics for use in inflatable structures.

The research documented in this report focuses on the mechanics of air-inflated drop-stitch fabric panels that are subject to bending loads. Both analytical and experimental methods were used: the results of experimental four-point bend tests conducted at various inflation pressures were used to validate the analytical method, and predicted and experimentally obtained data such as deflections, wrinkling onset moments, ultimate loads, and pressure changes were compared.

2. CHARACTERISTICS OF DROP-STITCH FABRICS AND AIR-INFLATED STRUCTURES

Drop-stitch fabrics, also known as spacer fabrics, are examples of three-dimensional (3-D) woven pre-forms (see figure 1); they consist of two skins (deck layers) that are simultaneously woven and spaced apart by a distance governed by the length of the drop yarns (also known as pile yarns). The drop yarns, which are a second family of warp yarns woven within the skins, are periodically "dropped" from one skin to the other skin and repeated in an alternating manner as shown in figure 1. For use in air-inflated structures, the skins are made impermeable by laminating them with layers of an elastomeric material, such as rubber, polyvinyl chloride (PVC), urethane, and neoprene, on both sides to fully contain a volume of air with their edges seamed. The skins consist of (1) a base fabric that is plain-woven using two orthogonal yarn directions referred to as the "warp" and "weft" directions and (2) a second warp yarn family for the drop yarns. The weft direction corresponds to the width direction and is limited by the size of the loom beam. The warp direction, referred to as the "direction of weaving," is virtually unlimited in length.

Figure 1. Example of a Drop-Stitch Fabric with Rubber-Laminated Skins

The load-carrying behavior of air-inflated drop-stitch panels is analogous to that of sandwich panels in which air acts as the foam (or honeycomb) core of a traditional sandwich panel and provides the through-thickness normal and transverse shearing stiffnesses. Load-carrying capacities and stability of inflatable drop-stitch panels depend on their shapes, fabric architectures, material properties, inflation pressures, mechanical loads, and temperature. Additionally, pressure relief valves and manifolding of inflation ports can be used to control the deployment and performance of drop-stitch panels used in inflatable structures.

The drop-stitch skins of the present research were constructed of a plain-woven, polyester fabric laminated with rubber layers on each surface. The warp, weft, and drop yarns are all constructed of polyester fibers. Figure 2 shows the base and laminated fabric construction details. The pure shearing behavior of rubber-coated woven fabrics is discussed in an experimental investigation.[11]

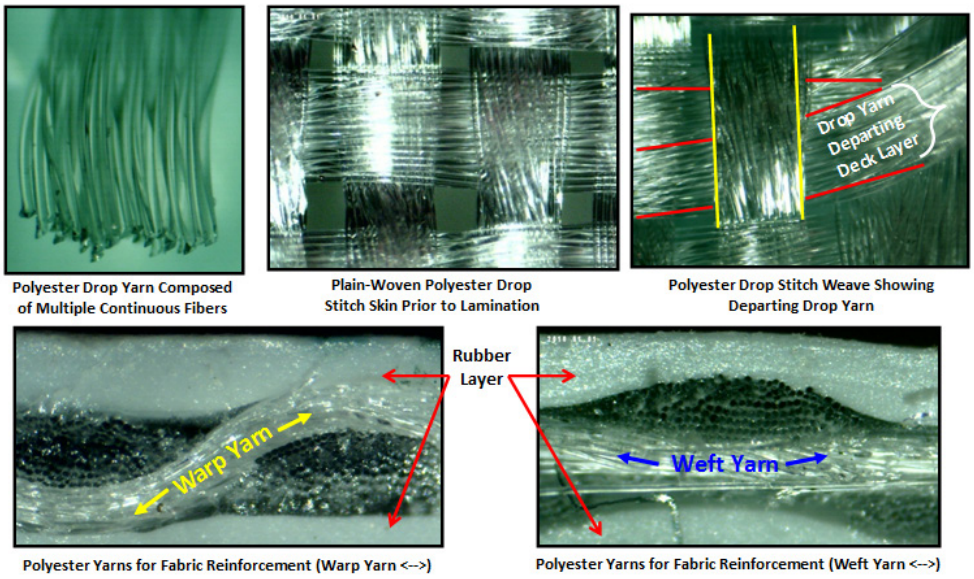

Figure 2. Construction Details of Rubber-Laminated, Polyester Fabric-Reinforced Drop-Stitch Skins

3. ANALYTICAL MECHANICS

During inflation of a drop-stitch panel, the air volume increases with pressure and a developable shape is produced. The skins become biaxially pretensioned, and the drop yarns become pretensioned to maintain the panel's flat shape. These pretensions produce the stiffnesses necessary for the panel to resist axial, bending, shear, and torsion loads.

Biaxial pretensioning is critical to the panel's ability to support loads. In general, sufficient bending stiffness can exist only along a particular direction if the pretension stresses from inflation in that direction have not been fully relaxed by opposing (compressive) stresses. Because the skins are thin compared to their planar dimensions, many researchers have assumed that the skins behave as tension-only membranes and therefore cannot resist in-plane compressive forces and cannot develop bending strain energies. In fact, however, because of the biaxial nature of the stress distributions from inflation, resistance to in-plane compressive stresses can exist along a direction having zero net tensile stress provided that there exists a tensile stress along the orthogonal in-plane direction. The theoretical maximum bending moment $M_{ultimate}$ is, therefore, approximately double the bending moment corresponding to the theoretical wrinkling onset moment M_{onset}.[1]

Air can be treated in accordance with the Ideal Gas Law, or,

$$PV = RT, \tag{1}$$

where P is the absolute pressure, V is the volume of air, R is the ideal gas constant, and T is the absolute temperature (°K). Additionally, for a polytropic thermodynamic process,[12] the pressure-volume relationship for the compression cycle of a gas as shown in figure 3 can be given as

$$PV^n = C, \tag{2}$$

where C = constant, and n = the ratio of specific heats (n = 1.4 for air).

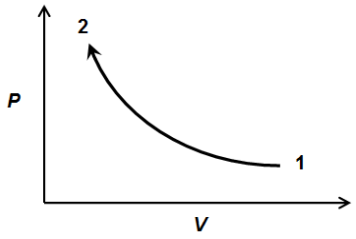

Figure 3. Compression Cycle for a Gas from State 1 to State 2

Two states of a polytropic compression (or expansion) process therefore can be described by

$$P_1V_1^n = P_2V_2^n. \tag{3}$$

Fluid-structure interactions (FSIs) occur when the enclosed air (fluid) experiences pressure and volume changes resulting from panel deformations due to applied mechanical and thermal loads. Additionally, tensile strains can develop in the membrane material which will, for a closed system, contribute to volume increases. This type of fluid-structure coupling, which is unique to inflated structures, is a source of nonlinear behavior. This coupling increases the complexity of the governing mechanics. When FSIs are significant, air compressibility must be included in the energy balance because, in addition to the strain energy developed in the membrane materials, the thermodynamic work done on the air, known as *PV*-work, must be accounted for.

The idealized form of the energy balance for an air-inflated fabric structure is

$$\int F d\delta = \Delta E_{\text{int}ernal} = \Delta E_{strain} + \Delta E_{kinetic} + \Delta E_{dissipative} + \Delta \int PdV + \Delta \int VdP, \tag{4}$$

where F is an externally applied force, δ is the deflection at point of loading, $E_{internal}$ is the internal energy of the system, E_{strain} is the sum of the elastic (recoverable) and plastic (irrecoverable) strain energies, $E_{kinetic}$ is the kinetic energy of the system mass, and $E_{dissipative}$ is the dissipated energy through damping and viscous effects. The Δ symbol is used to denote differences between inflated and bending states.

3.1 SHEARING DEFORMATIONS AS A SOURCE OF *PV*-WORK

The key source of volume change during four-point bending of an inflated drop-stitch panel prior to wrinkling and the loss of stability is the transverse shearing deformations of the cross section. Consider a panel constructed with inextensible skins that is subject to four-point bending as shown in figure 4 where β is defined as the angle between the neutral surface and a line initially perpendicular to the neutral surface. Region 1 is a region of pure bending in which no transverse shearing strain γ is present and β remains equal to $\pi/2$. Note that plane sections remain plane within this region. The volume within region 1 remains constant during bending, and no *PV*-work is produced in this region. Region 2, however, is subjected to a uniform transverse shearing strain that deforms the cross section, causing the plane sections to not remain plane so that β is no longer equal to $\pi/2$. The volume change due to γ in region 2 is equilibrated by a corresponding change in pressure that leads to *PV*-work; therefore, the effective shear modulus G_{eff} of the structure is a function of inflation pressure and γ. For the case of deformable skins, G_{eff} is a function of inflation pressure and the shear modulus of the skins G_{skins}.

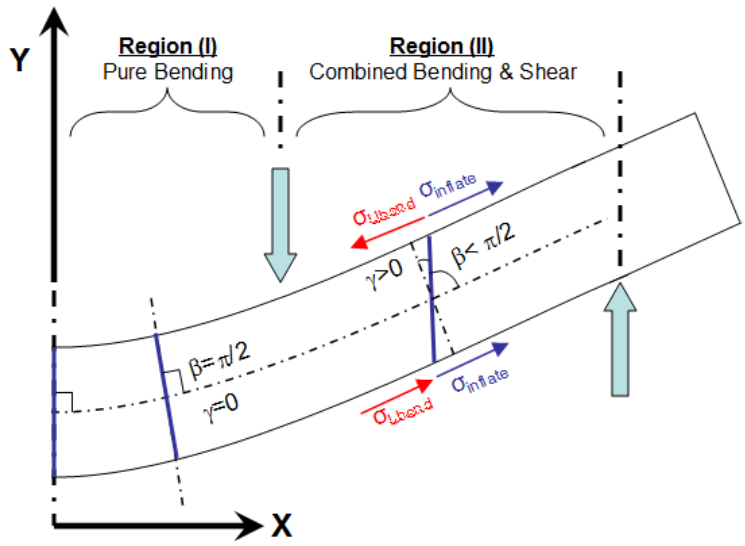

Figure 4. Superposition of Skin Stresses and Shearing Deformations

3.2 WRINKLING ONSET

The key to developing a specific load-carrying capacity and wrinkling stability level is balancing the applied stresses from external loading and the pretension stresses from inflation. The theoretical wrinkling onset occurs when a region of applied in-plane compressive stress completely relaxes the pretension stress in a given direction. Although full load-carrying capacity is available when the applied stresses have not fully relaxed the pretension stresses, the post-wrinkled, load-carrying capacity becomes reduced. This reduction depends on further loss of active cross section and eventual structural instabilities including buckling. The skins, however, are capable of resisting in-plane compression provided that the orthogonal direction remains under tension and therefore $M_{ultimate}$ is approximately double M_{onset}.

Wrinkling failures, which are a form of fail-safe collapse in air-inflated fabric structures, are preferred over yielding and fracture failures associated with materials used in conventional rigid structures. Wrinkling deformations can be readily and visually detected—unlike plasticity and crack growth, which may require other detection techniques. Today's inflatable structures can achieve significantly high, but safe and reliable operating pressures by using (1) continuous textile processing methods, which eliminates/reduces the number of seams, and (2) high-performance fibers.

3.3 WRINKLING STABILITY

Skin wrinkling is a phenomenon that occurs because of superposition of the bending stresses with the pretension stresses from inflation. During bending, as shown in the half-symmetry view of figure 5, compressive stresses are applied to the upper skin (point A) and tensile stresses are applied to the lower skin (point A′). The skin reaction forces create the

necessary force-couple required to resist the bending moment and maintain static equilibrium. The applied compressive stresses in the upper skin oppose (relax) the in-plane pretension stresses that are developed during inflation as shown in figure 6. The applied tensile stresses in the lower skin add to the in-plane pretension stresses from inflation. The bending moment that completely relaxes the pretension stress in the upper skin (so that the net longitudinal stress is zero) is referred to as "the wrinkling moment onset," M_{onset}, as shown in equation (5) for drop-stitch panels of the specific panel geometry described previously. Note that equation (5) is valid for skin thickness $t_{skin} << h$ so that higher ordered terms in t_{skin} are negligible. The inflated values of h and w_o are used (that is, $h(P_i)$ and $w_o(P_i)$) to capture the volume changes due to inflation. Skin wrinkling is fully developed at $M_{ultimate} \approx 2\ M_{onset}$, which occurs from a loss of the effective load-carrying cross section and, unlike in conventional rigid materials, is reversible in membrane skins.

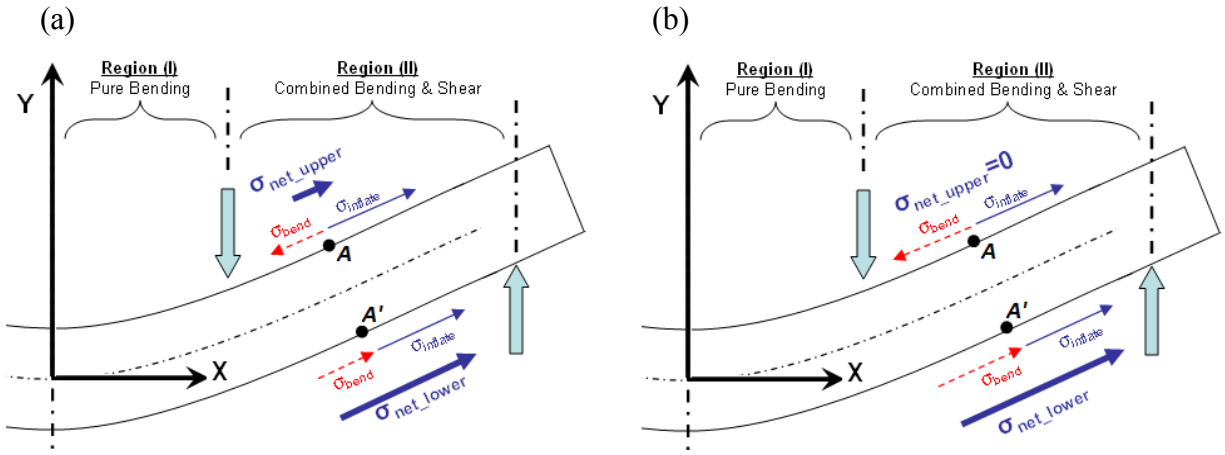

Figure 5. Superposition of Inflation and Bending Stresses (a) Prior to Wrinkling and (b) at Wrinkling Onset

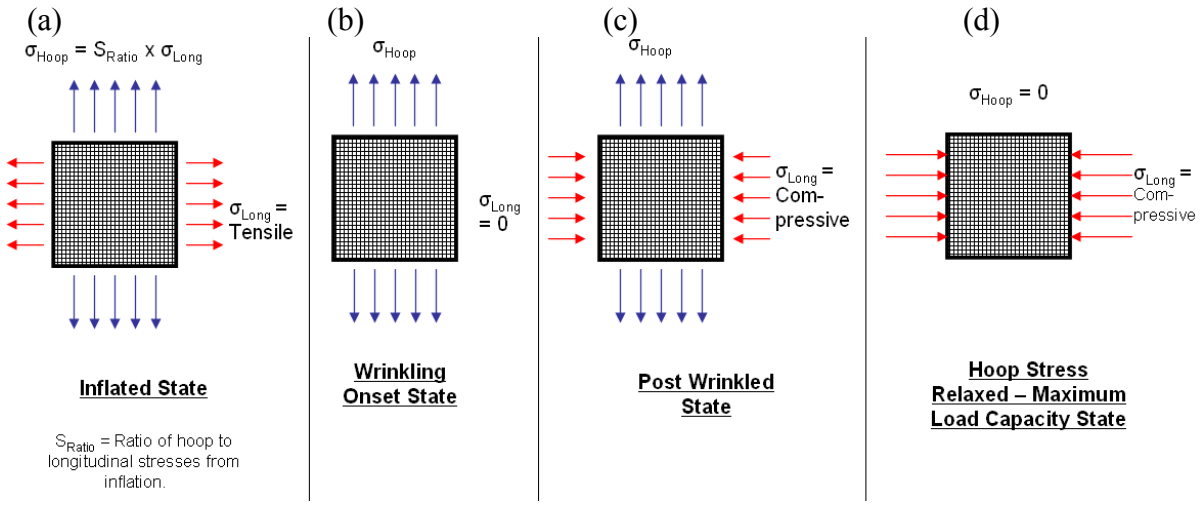

Figure 6. States of Superimposed Stresses on an Upper Skin Element

$$M_{onset} = \frac{P_i}{16} h(P_i)^2 \frac{(4w_o(P_i) - 4h(P_i) + \pi h(P_i))^2}{(2w_o(P_i) - 2h(P_i) + \pi h(P_i))}, \quad (5)$$

where h is the panel thickness, w_o is the panel width and P_i is the inflation pressure.

Wrinkling stability limits the load-carrying capacity of inflatable drop-stitch panels when the panels are subject to four-point bending loads. The structure simply loses stiffness when wrinkling develops; eventually, fail-safe collapse follows when $M_{ultimate}$ is reached. A fail-safe collapse does not generally damage the drop-stitch panel. Upon restoration of the panel to its pre-wrinkling load, the drop-stitch panel returns to its intended design shape.

3.4 DROP-STITCH PANEL GEOMETRY

The current air-inflated drop-stitch panel geometry is a nominally flat, enclosed volume with rounded edges as shown in figure 7. The overall panel length was L_o. The edges were radiused with a radius equal to $h/2$. The drop yarns were assumed to be uniformly distributed and were further assumed to possess extensional stiffness only; that is, the drop yarns provided no reaction forces due to net compressive forces. Note that, in fabricating drop-stitch panels of the given geometry, drop yarns within the vicinity of the radiused edges were assumed to be non-participatory because their effective lengths were restricted to be less than their straightened lengths and were assumed to remain slack for all time.

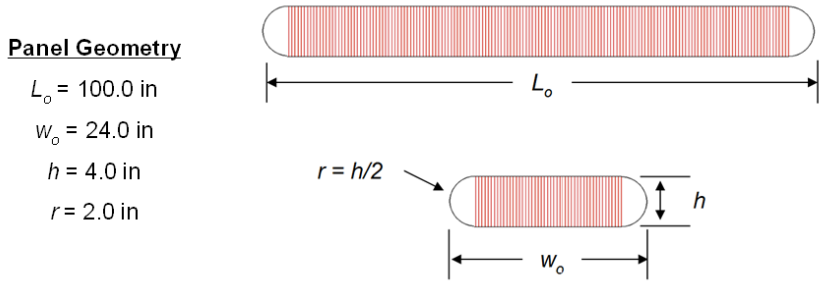

Figure 7. Geometry and Loading Parameters for Inflatable Drop-Stitch Panel

3.5 LOADING ARRANGEMENT

A four-point bending arrangement, rather than a three-point, was the preferred configuration for loading for the following reasons:

1. The four-point bending arrangement developed a region in which pure bending resided and no transverse shear stresses were present as shown in the shear and moment diagrams in figure 8.

2. The four-point bending arrangement provided an opportunity for wrinkling of the membrane material to occur remote from the loading points, which led to a greater wrinkling moment capacity than what would be obtained using three-point bending in which there was a high probability that wrinkling would develop at the load point.

The support and load point spans were the distances L_s and L_p, respectively. The moment arm was L_{arm}.

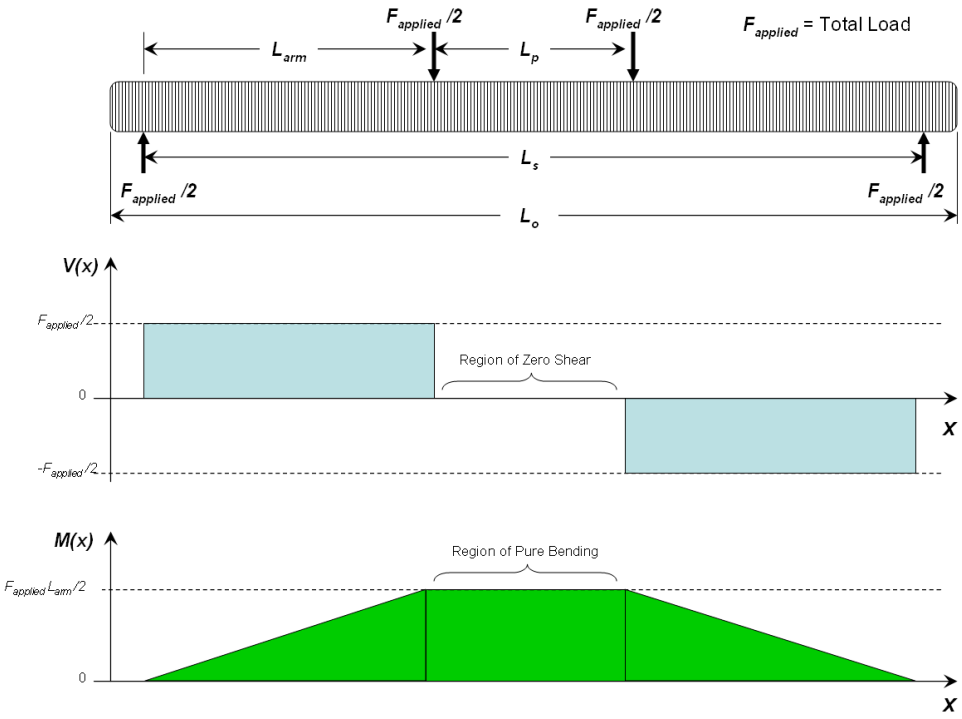

Figure 8. Four-Point Bend Loading Arrangement with Shear (V) and Moment (M) Diagrams

3.6 DEFLECTION ANALYSIS USING A SHEAR-DEFORMABLE BEAM THEORY

Unlike conventional structures, air-inflated structures stiffen with increasing pressure and are particularly sensitive to volume changes arising from transverse shearing deformations of their cross sections. The Euler beam theory (EBT) requires that plane sections remain plane. By doing so, EBT neglects transverse shearing deformations and therefore underestimates deflections of air-inflated beam-like structures—especially true when the inflatable structure operates at relatively low pressures. Furthermore, in addition to the shear modulus of the skin material, pressurized air also contributes to the transverse shear stiffness of an air-inflated structure. If the elastic and shear moduli of the skins are invariant over the range of inflation pressure considered prior to wrinkling, then the pressure-dependence on stiffness is in the effective shear modulus G_{eff} of the structure.

For the present panel dimensions and loading arrangement, values of G_{eff} were computed at the wrinkling onset for each inflation pressure listed in table 1. The use of a shear-deformable beam theory (SDBT), such as that by Timoshenko,[13] includes the effects of transverse shearing deformations on beam deflections and may be utilized to predict deflections of air-inflated beam-like structures. SDBTs establish beam deflections by superposition of two components: bending and shearing.

Table 1. Effective Shear Modulus, G_{eff}

Inflation Pressure P_i (psig)	**G_{eff} (psi)**	**G_{eff} P_i**
5.0	57.29	11.46
10.0	114.22	11.42
15.0	170.78	11.39
20.0	226.98	11.35
25.0	282.83	11.31
30.0	338.31	11.28
35.0	393.45	11.24
40.0	448.23	11.21

An SDBT is now developed in which the pressure-dependent values of E_{skin} and G_{eff}, which represent the skin elastic modulus (measured along the longitudinal axis of the panel) and the effective transverse shearing modulus of the air-filled panel, correspond to the current inflation (gage) pressure P_i and are assumed to be invariant during the bending event.

Using Castigliano's second theorem,[14] the pressure-dependent, total strain energy $U_{total(P_i)}$ is expressed as the sum of the bending strain energy of the skins and the shearing strain energy of the panel's cross-sectional area A, as shown in equation (6)

$$U_{total}(P_i) = \int_0^{L_s} \frac{M(x)^2}{2E_{skin}(P_i)I}dx + \int_0^{L_s} FS\frac{V(x)^2}{2G_{eff}(P_i)A}dx, \tag{6}$$

where

x = position along the supported span length,

$E_{skin}(P_i)$ = skin elastic modulus at current inflation pressure,

$G_{eff}(P_i)$ = effective transverse shearing modulus at current inflation pressure,

I = second area moment of inertia of the cross section as defined by the skins with respect to the neutral axis, and

FS = shear strain correction factor.

The total pressure-dependent, midspan deflection $\delta_{total}(P_i)$ resulting from the total applied four-point bending load $F_{applied}$ is derived by minimizing $U_{total}(P_i)$ with respect to x, which leads to the following SDBT solution:

$$\delta_{total}(P_i) = \frac{F_{applied}\, L_{arm}\left[3\left(\frac{L_s}{2}\right)^2 - L_{arm}{}^2\right]}{E_{skin}(P_i)\, w_o\left[h^3 - (h-2t_{skin})^3\right]} + \frac{3\,F_{applied}\, L_{arm}}{5\,G_{eff}(P_i) w_o\,(h-2t_{skin})}, \tag{7}$$

in which the first and second terms in equation (7) represent the bending and shearing components, respectively, of the total midspan deflection.

3.7 MECHANICS OF DROP-STITCH PANELS SUBJECT TO FOUR-POINT BENDING

Four-point bending loads applied to an air-inflated drop-stitch panel of the geometry previously described produces longitudinal tensile stresses in the lower skin and longitudinal compressive stresses in the upper skin (see figure 4). The infinitesimal element length indicated in figure 4 demonstrates the balance of pretension and applied bending stresses.

Now consider the inflation step. As air fills the volume enclosed by the skins, the biaxial pretension stresses develop along the length and width directions in such a way that static equilibrium is achieved and the panel attains its developable shape. Once the panel is pressurized, the longitudinal force $F_{longitudinal}$ is computed as the product of inflation pressure and longitudinal projected area:

$$F_{longitudinal} = P_i\left[(w_o - h)h + \pi\frac{h^2}{4}\right]. \tag{8}$$

Similarly, the hoop force F_{hoop} is computed as the product of pressure and hoop projected area:

$$F_{hoop} = P_i\left[(L_o - h)h + \pi\frac{h^2}{4}\right]. \tag{9}$$

The longitudinal and hoop pretension stress resultants N_x and N_y, respectively, reported in conventional textile force-per-unit-length notation are

$$N_x = F_{longitudinal} / [2(w_o - h) + \pi h], \text{ and} \tag{10}$$

$$N_y = F_{hoop} / [2(L_o - h) + \pi h], \tag{11}$$

where x and y are orthogonally aligned along the longitudinal and width directions, respectively. The denominators of equations (10) and (11) represent the perimeters of the longitudinal and hoop cross sections, respectively. The stress resultants are important because they can be directly compared to strengths obtained through tensile tests (also reported in force-per-unit-length notation) performed on the skin materials to establish factors of safety (FOS) on tensile rupture.

Equations (10) and (11) can be easily converted to obtain engineering stresses σ_x and σ_y with units in force-per-unit area by simply dividing each engineering stress by the skin thickness t_{skin}:

$$\sigma_x = N_x / t_{skin} = F_{longitudinal} / \left[\left(2\left(w_o - h \right) + \pi h \right) t_{skin} \right], \text{ and} \tag{12}$$

$$\sigma_x = N_y / t_{skin} = F_{hoop} / \left[\left(2\left(l_o - h \right) + \pi h \right) t_{skin} \right]. \tag{13}$$

The shape of the inflated structure affects the ratio of biaxial tensile forces per unit length N_{ratio} developed during pressurization and is expressed as

$$N_{ratio} = N_y / N_x . \tag{14}$$

For a right circular cylinder, $N_{ratio} = 2.0$. For the drop-stitch panel of the present dimensions ($L_o = 100''$, $w_o = 24''$, $h = 4.0''$, and $t_{skin} = 0.096''$), $N_{ratio} = 1.1$.

Volume changes due to the inflation of drop-stitch panels arise from the extensibility of the skins and drop yarns. If the elastic moduli are known for the skins and drop yarns, then the volume change upon inflation, which is simply the result of the strains developed in the skins and drop yarns, can be readily computed. Strains in the skins increase the longitudinal and hoop perimeters of the skins. Similarly, strains in the drop yarns increase the drop-yarn lengths, which also increase the panel thickness and volume.

The present analytical solution assumes that the spatial density of the drop yarns, defined as the number of drop yarns per unit area, is sufficient, so that localized skin bowing deformations between adjacent drop yarns have a negligible effect on volume changes. Note that volume changes increase with decreasing drop-yarn densities for a given pressure. Furthermore, the present analysis provides a total solution by considering (1) pressure and volume changes with respect to inflation and (2) pressure and volume changes with respect to applied loads.

4. EXPERIMENTAL MECHANICS

4.1 MATERIAL PROPERTY TESTS

The analytical models require material property data as input. Skin strains caused by inflation are computed using elastic moduli obtained through experimental tensile tests. Biaxial tension testing is the preferred method for characterizing the strength and elastic moduli of membrane skins used in inflatable structures because of the skins' biaxial pretensioning from pressure. Although a fixture[15] of the type shown in figure 9 is recommended for its capacity to independently apply different tensile stress ratios with combined shearing, one was not available at the time of this research.

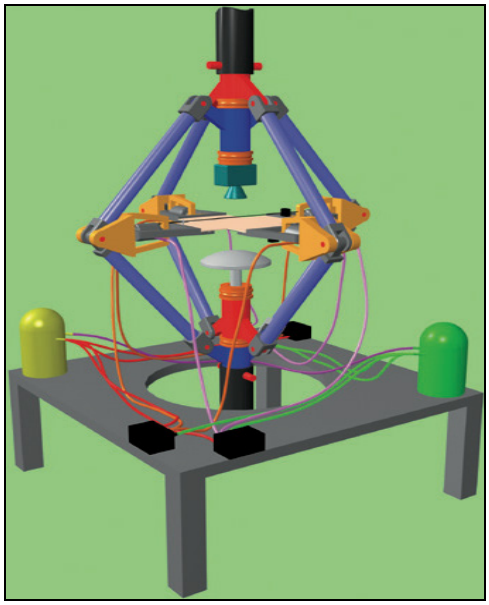

Figure 9. Advanced Biaxial Tension and Combined Shear Test Fixture with Proportional Tension Controls (U.S. Patent 7,204,160[15])

Ideally, the ratio of biaxial tension stresses used in the test should match the ratio of biaxial tension stresses N_{ratio} produced in the actual structure from inflation. The ratio of biaxial tension stresses is dependent on the geometry of the inflated structure. In the absence of biaxial testing capability, uniaxial tensile tests can be performed and stress stiffening effects from biaxial loading can be established for an isotropic material having an effective elastic modulus, E_{eff} and Poisson's ratio ν as shown in equation (15). The effective modulus from biaxial stress stiffening is computed by combining equations (12) through (14) with the plane stress form of Hooke's law shown in equation (16).

$$E_{eff} = E_{skin} / (1 - N_{ratio} \nu), \tag{15}$$

where E_{skin} is the elastic modulus of the skins obtained from uniaxial tension tests, and ε_x is the axial strain:

$$\varepsilon_x = \frac{1}{E_{skin}}\left(\sigma_x - \nu\sigma_y\right). \tag{16}$$

The uniaxial tensile test method was used in this research: the rubber-laminated polyester skin specimens were cut from as-fabricated drop-stitch panels and tested using an Instron machine as shown in figure 10. Note that the polyester drop yarns were cut at their midlength and were allowed to hang freely. The resulting stress, instantaneous elastic modulus E_{inst} and effective elastic modulus E_{eff} versus strain curves are shown in figures 11 – 13. Figure 13 exhibits the pressure stiffening effect on E_{eff} and was determined through consideration of E_{skin}, ε_x, and N_{ratio}.

Figure 10. Tensile Testing of Drop-Stitch Skin Materials

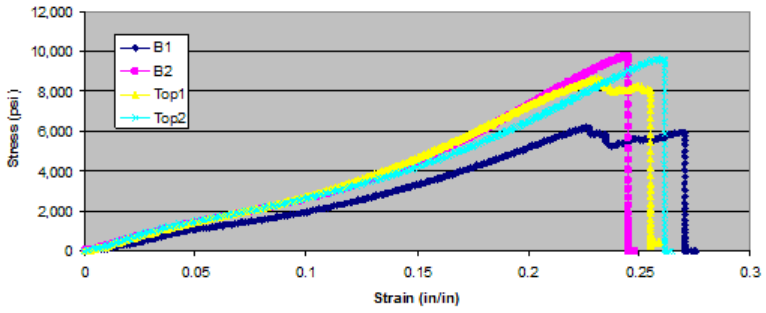

Figure 11. Stress Versus Strain Curves for Drop-Stitch Skin Tensile Test Specimens

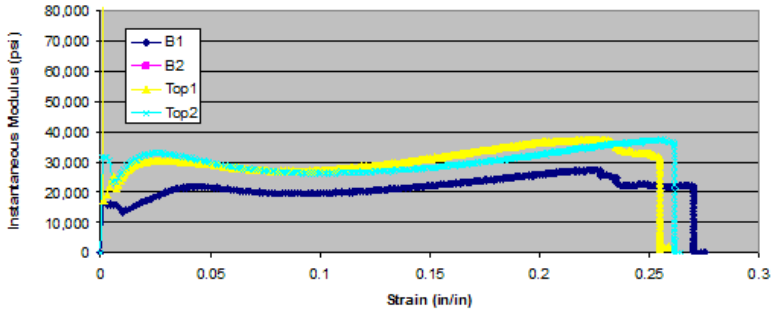

Figure 12. Instantaneous Elastic Modulus E_{inst} Versus Strain Curves for Drop-Stitch Skin Uniaxial Tensile Test Specimens

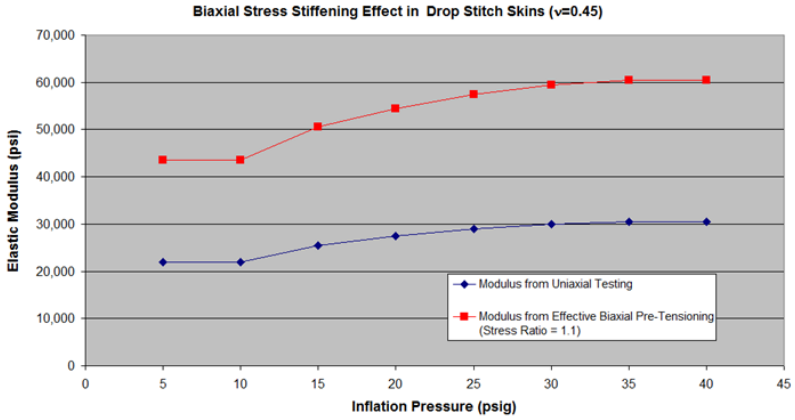

Figure 13. Instantaneous Elastic Modulus E_{inst} and Effective Elastic Modulus E_{eff} Versus Inflation Pressure for Drop-Stitch Panel Test Specimen

An average elastic modulus of the skins was established from the instantaneous modulus versus strain curves and was used to represent the elastic modulus for both the warp and weft directions. If the warp and weft elastic moduli of the skins are different, then the material should be treated as orthotropic and the appropriate elastic moduli should be used in their corresponding directions. The average elastic modulus is justified for use in analytical solutions when the applied bending stresses can be considered to be a perturbation about the inflated stress state.

In a similar fashion, it was necessary to characterize the tensile properties of the drop yarns including their failure modes, failure strengths, elongations at break, and elastic moduli. Tensile properties of the drop yarns were established using two methods. The first method conducted tensile tests directly on individual yarns in both pre-woven and post-woven states (for the latter, yarns were extracted from the drop-stitch fabric before lamination) as shown in figure 14 (a) to establish the effects of yarn damage from weaving on their strength and stiffness.

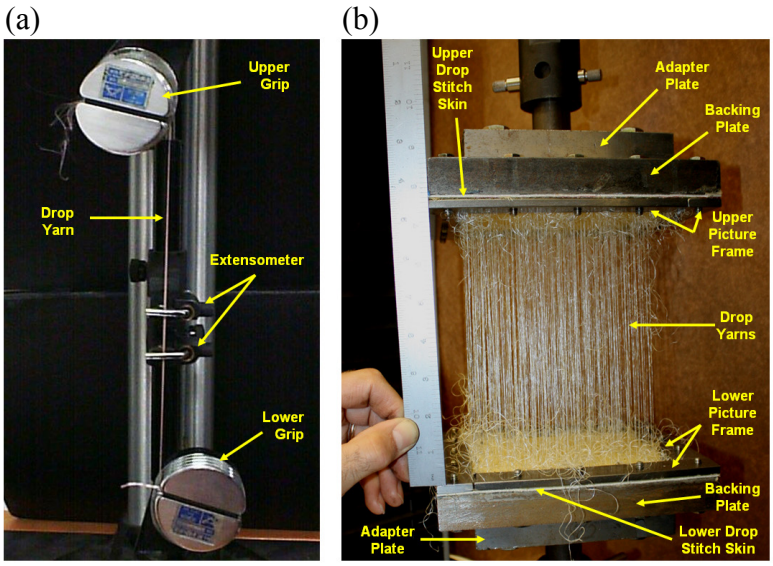

Figure 14. (a) Tensile Testing of Individual Drop Yarns and (b) Tensile Testing of Drop Yarns in Woven State

A second method was developed to obtain the tensile strengths of the drop yarns while incorporating the drop stitch as a complete, 3-D woven laminated system. The purpose was to determine if the woven architecture of the drop-stitch skins and the lamination layers had any influence on the tensile strengths and failure modes of the drop-stitch yarns. If the drop yarns failed remotely from the skins (that is, at the midlength of the drop yarn), then the skins had no effect on the drop-yarn tensile strengths and failure modes. If, however, the drop yarns failed at the region of egress from the skins, then their tensile properties could be influenced by the woven architecture of the skins (that is, yarn counts per unit length of skin, crimp contents, etc.) and the ability of the skins to prevent pull-through of the drop yarns from the skins. This test required the design of a novel test fixture for use in a conventional strength of materials test machine. The device, shown in figure 14 (b), incorporated a 6- by 6-inch swatch of the drop-stitch fabric that was adhesively bonded to a pair of steel backing plates. A series of 1-inch-wide plates was used to form picture frame assemblies that were bolted around the perimeter of each skin. The picture frames were necessary to eliminate peel stress failures of the adhesive bond layers and to promote uniformity of the drop-yarn tensions across the 6- by 6-inch region.

The polyester drop yarn properties listed in table 2 were characterized through measurements performed on scanning electron microscopy (SEM) images of extracted drop yarns. The weight density of polyester used to further compute the drop-yarn denier was 0.048 lb/in^3.

Table 2. Measured Properties of Polyester Drop Yarns

Property	Measured Value
No. of Fibers Per Drop Yarn	34
Average Fiber Diameter	25 microns
Average Fiber Area	7.609 E-07 $in.^2$
Average Drop Yarn Area	2.587 E-05 $in.^2$
Linear Mass Density	200 denier

Figure 15 shows the load-versus-strain curves obtained from uniaxial testing of individual polyester drop yarns extracted from the fabric, and figure 16 shows a fibril fracture mode of individually tested drop yarns. The resulting stress-versus-strain curves for the three polyester drop yarns (figure 15) are shown in figure 17. Assuming linear elastic behavior, the average elastic modulus of the drop yarns E_{dy} was 1.05 E + 06 psi.

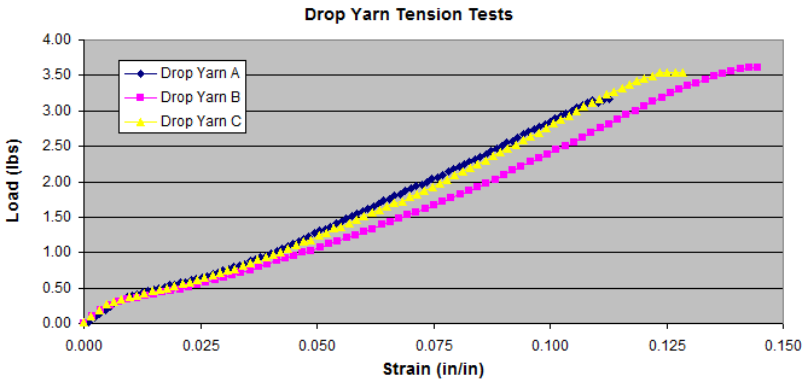

Figure 15. Load Versus Strain Curves Obtained from Uniaxial Testing of Individual Polyester Drop Yarns Extracted from the Fabric

Figure 16. Fibril Fracture Mode of Individually Tested Drop Yarns

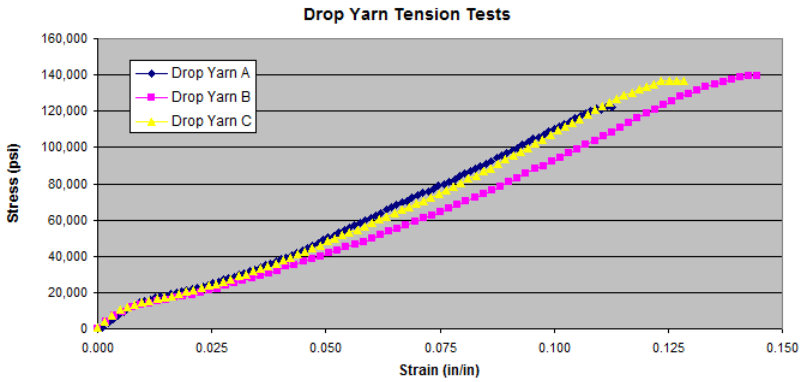

Figure 17. Stress Versus Strain Curves for Three Polyester Drop Yarns

4.2 FOUR-POINT BEND TESTS

Experimental four-point bend tests were conducted using an Instron machine configured with a customized, rigid test frame as shown in figure 18 on drop-stitch panels as described in figure 8 with L_o = 100 in., L_s = 76 in., L_p = 24 in., L_{arm} = 26 in., and t_{skin} = 0.096 in.

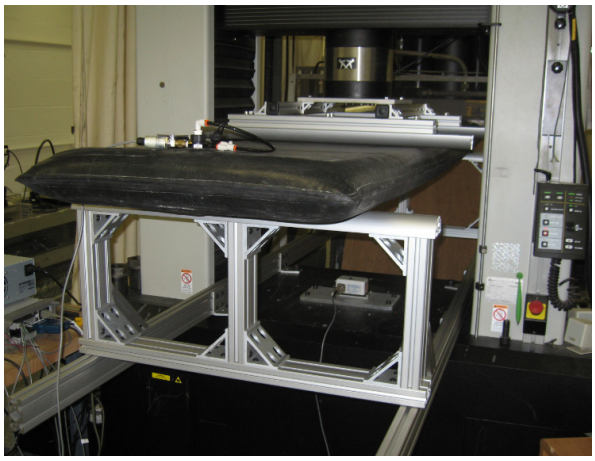

Figure 18. Experimental Four-Point Bend Test Arrangement

The bend tests were performed in displacement control mode at a constant crosshead rate of 1.0 inch/minute. The panels were inflated to each of the prescribed initial inflation pressures, and the air fill-valve was then turned off so that the air volume was a closed volume during the bending event. For safety purposes, however, a pressure relief valve was connected to the air fill-line.

Data recorded during each test included initial inflation pressure, instantaneous pressure, midspan deflection (using a displacement wire transducer), instantaneous load, load-point (crosshead) displacement, and temperature.

The panels were subjected to a series of initial bending cycles for preconditioning purposes to remove any alignment anomalies such as temporary curvature of the panels. These cycles consisted of three consecutive runs to achieve a 4.0-inch midspan deflection. The specimens were then flipped over, and three additional, similarly applied runs were performed.

After preconditioning was completed, three bend tests were conducted at each pressure. Loading ceased when the midspan deflection reached approximately 6.0 inches. No measurable changes in air temperature were observed. Figures 19 – 24 show graphs of total applied load versus midspan deflection for initial inflation pressures of 5, 10, 15, 20, 25, and 30 psig. The dotted line represents the analytical SDBT solution. The white circle designates the SDBT solution at the onset of wrinkling M_{onset}; the red circle designates the SDBT solution at the ultimate wrinkling moment $M_{ultimate}$.

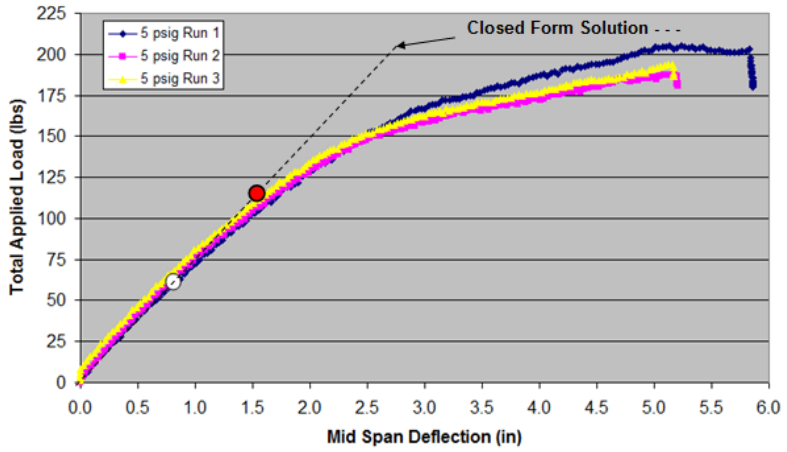

Figure 19. Load Versus Midspan Deflection for 5.0- psig Inflation

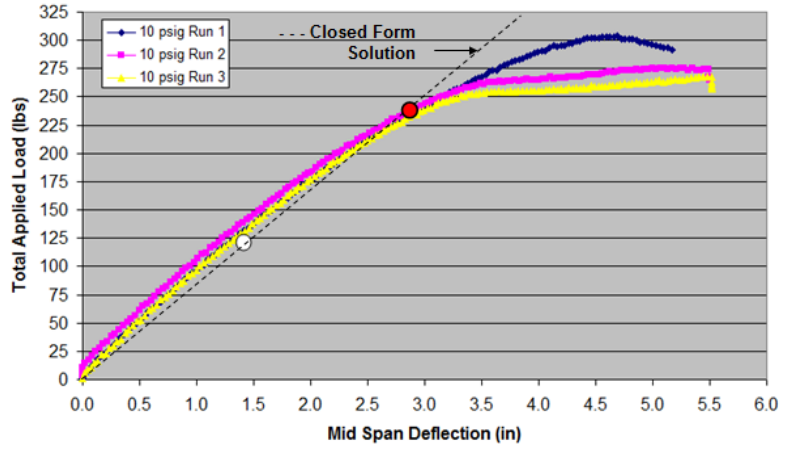

Figure 20. Load Versus Midspan Deflection for 10.0-psig Inflation

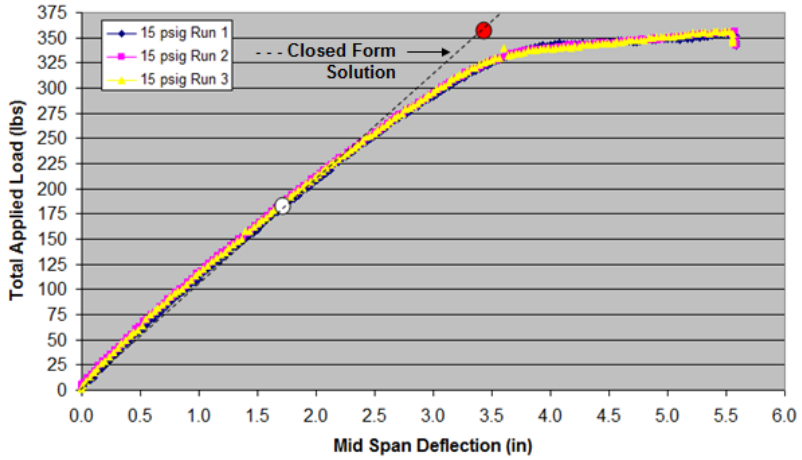

Figure 21. Load Versus Midspan Deflection for 15.0-psig Inflation

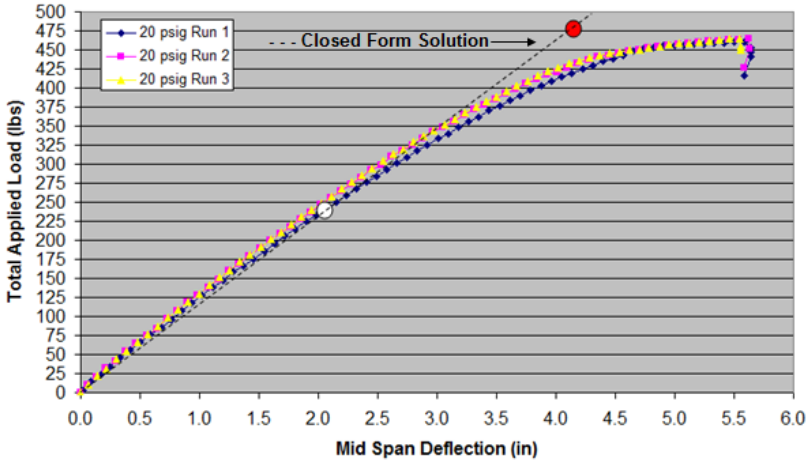

Figure 22. Load Versus Midspan Deflection for 20.0-psig Inflation

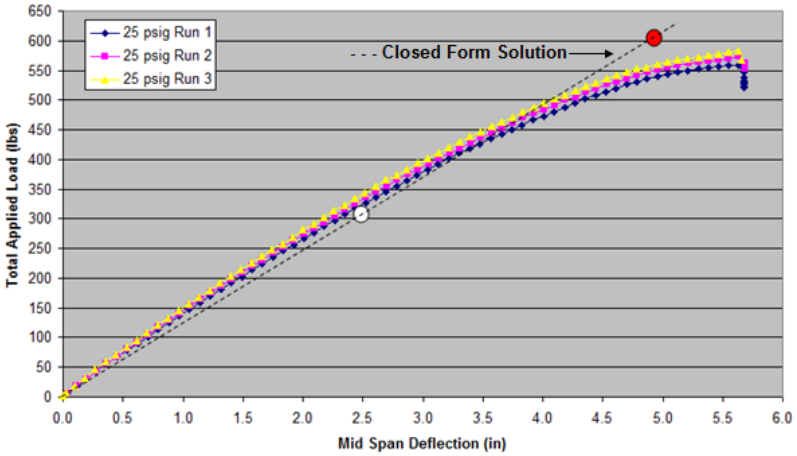

Figure 23. Load Versus Midspan Deflection for 25.0-psig Inflation

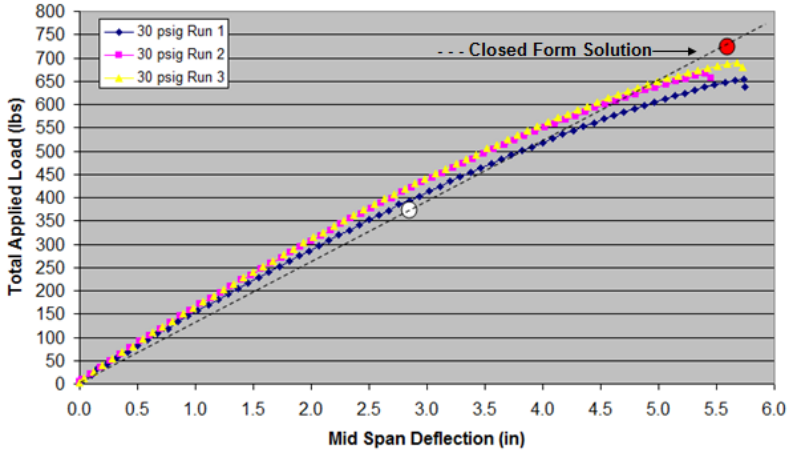

Figure 24. Load Versus Midspan Deflection for 30.0-psig Inflation

The onset of wrinkling was typically observed during the bend tests as the formation of a local creasing deformation extending across the full width of the upper skin adjacent to the outboard side of the load point (see figure 25).

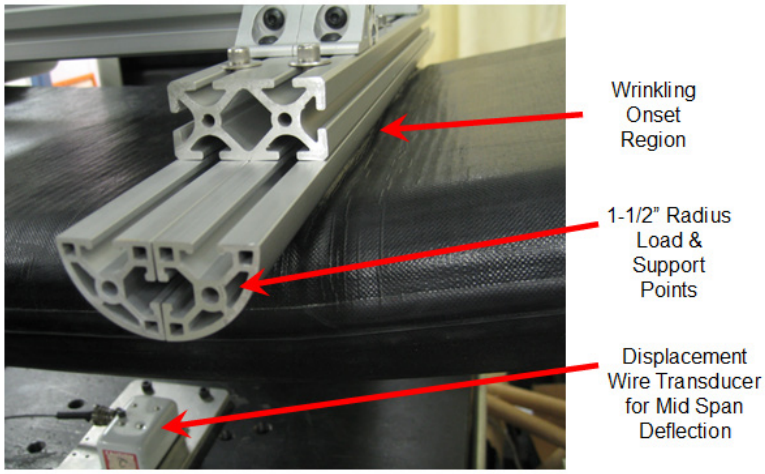

Figure 25. Example of the Wrinkling Onset Deformations in the Upper Skin Adjacent to the Outboard Side of the Load Point

Table 3 compares the pressure changes during the bending tests with the SDBT predictions at the wrinkling onset points shown in figures 19 – 24.

Table 3. Pressures at Bending at M_{onset}

Initial Pressure P_i	5.0	10.0	15.0	20.0	25.0	30.0
SDBT Pressure at M_{onset}	5.04	10.09	15.14	20.19	25.24	30.29
Experimental Pressure at M_{onset}	5.02	10.02	15.02	20.04	25.05	30.07

5. CONCLUSIONS

The pressure-dependent behavior of inflatable drop-stitch panels subject to four-point bending loads was investigated through combined analytical and experimental methods. The analytical method, developed using SDBT, accounted for (1) pressure and volume changes due to inflation and (2) pressure and volume changes due to applied bending loads.

Material level tests on the drop yarns and skins were performed to characterize their extensibility behaviors. The biaxial tensile behavior of the skins was established using Hooke's law in conjunction with uniaxial tensile test results. The panel geometry and biaxial tension ratio from inflation were shown to critically influence the SDBT solution.

Excellent correlation of load-deflection results was obtained between the SDBT predictions and the experimental results up to the wrinkling onset level for all inflation pressures. The SDBT predictions, however, underestimated the ultimate bending moment for pressures of 10 psig and below. This underestimation likely resulted from the inability of the drop-stitch panel to fully develop a symmetric loading state at such low pressures. The SDBT predicted slightly greater pressures at the wrinkling onset state than those measured during testing; however, the measured pressure changes up to the wrinkling onset were less than 0.4%.

The maximum applied experimental load at 30 psig was nearly 700 lb with a corresponding ultimate moment of 9100 in-lb—clearly demonstrating the significant load-carrying capacity of inflatable drop-stitch fabric panels. Based on the breaking strength of the drop yarns, however, the analytically predicted maximum achievable pressure was approximately 50 psig with a corresponding ultimate wrinkling moment of 16,152 in-lb and a total applied load of 1300 lb. The weight of the experimental panel was 22 lb resulting in a theoretical ultimate load-carrying ratio of 59:1. Such a ratio could be easily increased by using drop yarns of higher deniers (that is, increased filament counts) and higher tenacity fibers.

The panels used in this research were inflated over a range of safe operating pressures; no testing was performed to establish their burst pressures. However, assuming that the strengths of the skins and seamed edges exceeded the tensile strengths of the drop yarns, the expected mode of initial failure was drop-yarn tension failure. If drop-yarn tensile failures occur, air volume increases, panel deformations become cylindrical, pressure simultaneously drops, and stresses in the skins and remaining active drop yarns are redistributed— providing a unique margin of safety against total structural failure in addition to the wrinkling fail-safe mechanism.

The scope of this research is being expanded to include numerical solutions (finite element analysis) for predicting the post-wrinkled behavior through complete collapse and for inflatable drop-stitch fabric skins having significant hyperelastic behavior. Numerical solutions are most appropriate when nonlinearities due to geometric (large deflections, large strains, and large rotations) and material behavior are present. Such solutions can readily incorporate hyperelastic strain energy potentials (for example, Ogden[16] and Marlow[17]) to characterize their stiffness over a large range of bending stresses to preclude being restricted to perturbations about the inflated state. Additionally, the effects of drop-yarn tensile failures and local stress redistributions due to overpressurization will be investigated.

6. REFERENCES

1. P. S. Bulson, "Design Principles of Pneumatic Structures," *The Structural Engineer*, vol. 51, no. 6, June 1973.

2. M. Stein, J. M. Hedgepeth, "Analysis of Partly Wrinkled Membranes," Technical Note D-813, NASA Langley Research Center, Hampton, VA, July 1961.

3. W. Fichter, "A Theory for Inflated Thin-Wall Cylindrical Beams," NASA Technical Note D-3466, National Aeronautics and Space Administration, Washington, DC, 1966.

4. E. C. Steeves, "Behavior of Pressure Stabilized Beams Under Load," Technical Report 75-082-AMEL, United States Army Natick Development Center, Natick, MA, 1975.

5. P. Cavallaro and A. Sadegh, "Air-Inflated Fabric Structures," *Marks' Standard Handbook for Mechanical Engineers*, 11th edition, McGraw-Hill, NY, pp. 20.108 – 20.118, 16 November 2006.

6. P. Cavallaro, M. Johnson, and A. Sadegh, "Mechanics of Plain-Woven Fabrics for Inflated Structures," *Composite Structures Journal*, vol. 61, pp. 375 – 393, 2003.

7. P. Cavallaro, A. Sadegh, and C. Quigley, "Decrimping Behavior of Uncoated Plain-Woven Fabrics Subjected to Combined Biaxial Tension and Shear Stresses," *Textile Research Journal*, pp. 403 – 416, vol. 77, no. 6, 2007.

8. P. Cavallaro, A. Sadegh, and C. Quigley, "Contributions of Strain Energy and PV-Work on the Bending Behavior of Uncoated Plain-Woven Fabric Air Beams," *Journal of Engineered Fibers and Fabrics*, pp. 16 – 30, vol. 2, no. 1, 2007.

9. J. Falls and J. Waters, "Bending Tests of Inflatable Dropstitch Panels," *11th International Conference on Fast Sea Transportation, FAST 2011*, Honolulu, HI, September 2011.

10. J. Waters and J. Falls, "Bending Tests of Inflatable Dropstitch Panels," (draft), U.S. Naval Academy, 2010.

11. S. Farboodmanesh, J. Chen, J. L. Mead, and K. White, "Effect of Construction on Mechanical Behavior of Fabric Reinforced Rubber," *Rubber Division Meeting, American Chemical Society*, Pittsburgh, PA, 8 – 11 October 2002.

12. K. Wark, *Thermodynamics*, McGraw-Hill Book Co, 3rd edition, 1977.

13. S. Timoshenko, *Strength of Materials Parts 1&2*, Krieger Publishing Co, 3rd edition, 1983.

6. REFERENCES (Cont'd)

14. A. Ugural and S. Fenster, "Advanced Strength and Applied Elasticity," Elsevier North-Holland Publishing Co, 2nd edition, 1977.

15. P. Cavallaro, C. Quigley, and A. Sadegh, "Biaxial and Shear Testing Apparatus with Proportional Force Controls," U.S. Patent 7,204,160, 17 April 2007.

16. R. Ogden, "Non-Linear Elastic Deformations," Dover Publications Inc., July, 1997.

17. R. Marlow, "A General First-Invariant Hyperelastic Constitutive Model," *Constitutive Models for Rubber III*, Busfield and Muhr (eds.), Swets & Zeitlinger, Lisse, The Netherlands, 2003.

INITIAL DISTRIBUTION LIST

Addressee	No. of Copies
Office of Naval Research (ONR-331 (Kelly Cooper), ONR-332 (Y. Rajapakse), ONR-334 (R. Barsoum), ONR-DOI (L. Schuette))	4
U.S. Army Natick Soldier Research Center, Natick, MA (AMSRD-NSC-CP-CE (S-145) (G. Proulx, K. Buehler, C. Quigley, J. Hampel), AMSSB-RCP-C (M. Jee, J. Roche, J. Cullinane), AMSSB-RAD-D(N) (G. Thibault, R. Benny, T. Godfrey, M. Roylance))	11
Army Research Laboratory Weapons and Materials Research Directorate (AMSRL-WM-MB (R. Dooley, E. Chin))	2
U.S. Army Engineer Research and Development Center, Coastal and Hydraulics Laboratory (J. Melby, J. Fowler)	2
U.S. Army Research Office (L. Russell, Jr.)	1
NASA Langley Research Center	2
NASA Johnson Space Center	2
Navy Clothing and Textile Research Facility, Natick, MA (B. Avellini, A. Brayshaw, L. Caulfield, T. Hart, C. Heath)	5
United States Naval Academy (J. Waters, J. Falls)	2
Defense Technical Information Center	1
Center for Naval Analyses	1
Navatek Ltd.	2
The City College of the City University of New York	1
Cooley/Group	1
Warwick Mills	1
Federal Fabrics-Fibers	2
ILC Dover	4
Hunter Defense Technologies	1